1993-11

Measurement of submicrometer Al2O3 particles in plumes

Kim, H.-O.

Measurement of submicrometer Al_2O_3 particles in plumes

H.-O. Kim, D. Laredo, and D. W. Netzer

We made multiple-wavelength light transmission measurements at the edge of a plume from a small solid-propellant motor in order to determine the mean particle size and the *in situ* particle index of refraction. We retrieved the particle size distribution from the Sauter mean diameter and the geometrical standard deviation assuming a lognormal distribution. The good correlation of the data indicated the applicability of the technique with a relatively high confidence level and that submicrometer particles were dominantly present at the edge of the plume. This was confirmed by the size distribution of collected particles. The values measured for alumina particles in the edge of the plume were a Sauter mean diameter of 0.150 μm ± 4%, a geometrical standard deviation of 1.50 ± 3%, and a real index of refraction of 1.63 ± 8%.

Key words: Aluminum oxide, plume signature, particle size, particle optical properties.

Introduction

One can use metal fuel additives such as aluminum in solid-propellant rocket motors to achieve high specific impulse. Besides causing performance losses in the nozzle, the condensed Al_2O_3 particles are the major source of primary smoke in the exhaust plume. The particulate matter can also have major effects on the plume IR signature. High number densities of particles can block gas-phase radiation from the plume. They can also be the source of radiation, especially the larger particles that exit the nozzle not in thermal equilibrium with the gas. The detection, identification, tracking, and targeting of missiles that employ these propellants are all important issues in the development of space defense systems.

The prediction of plume signature is currently accomplished by using codes such as the Standardized Plume Flowfield (SPF) model and the Standardized Infrared Radiation model (SIRRM).[1] One can use the nozzle/plume flow-field codes[1,2] to predict that the particle size distribution within the plume is not uniformly distributed in the radial direction. If particles exist in the plume that are larger than approximately 5 μm, they will be concentrated along the plume centerline, failing to follow the rapid gas flow turning that occurs in the nozzle throat region. Even particles as small as 1.0 μm are predicted not to follow the flow along the diverging nozzle wall. There is also experimental evidence that most of the number of Al_2O_3 particles in plumes are less than 1 μm in diameter.[3–5] Thus it is expected that particles in the outer regions of the plume will be less than 1.0 μm in diameter. The smaller particles are generally predicted to be in thermal equilibrium with the surrounding gas. Thus if the equilibrium exhaust temperature from the nozzle is less than 2318 K (alumina melting point), it is reasonable to assume that the smaller particles are solids. The larger molten particles are limited to the central region of the plume. Solid Al_2O_3 is known to have considerably lower emittance than liquid Al_2O_3. Thus if small solid particles dominate the outer regions of the plume, they can have a dominant effect on the plume signature.

The particle size distribution, particle concentration, and particle optical properties all have considerable influence on the plume signature. Both the prediction of plume signature and the measurement of particle size distributions within the plume depend on an accurate knowledge of the particle optical properties, especially the particle complex refractive index. For aluminum oxide the refractive index is generally between 1.65 and 1.85. Larger particles are dominated by the alpha phase with a higher refractive index, whereas the smaller particles are generally gamma phase with a lower refractive index.[5,6] The absorption coefficient has been reported[7] to be between 10^{-2} and 10^{-7}. These properties may

The authors are with the Naval Postgraduate School, Monterey, California 93943-5000.

Received 24 February 1992.
0003-6935/93/336834-07$06.00/0.

also be dependent on the thermal history of the particles.[5] Small amounts of contaminants can also apparently have a significant effect on the refractive index. This is of importance in rocket motor plumes since contaminants such as soot are present and the rapidly changing temperatures can result in various phases of aluminum oxide being present. Larger booster motors use propellants with 14–20% aluminum by weight, resulting in 25–38% of the exhaust being condensed Al_2O_3. These plumes are optically thick, making optically based particle sizing diagnostic techniques difficult to employ.

The objective of the investigation was to measure the mean particle size and *in situ* particle index of refraction in the outer region of the plume of a small solid-propellant rocket motor. The technique that we employed was multiple-wavelength light transmission measurements together with the use of a Mie code for obtaining the mean extinction coefficients as a function of the particle size distribution, index of refraction, and wavelengths of the illumination source. This technique is limited[8] to particles smaller than approximately 1.0 μm when UV and/or visible light is used. We used a collimated mercury light source to provide five distinct wavelengths that were individually recorded within a spectrograph. We also used a helium–neon laser. We also investigated measurement sensitivity to the experimental variables.

We compared the particle size distribution obtained optically to SEM pictures of collected particles on a micropore filter (0.25-μm mesh). The collection of the particles from the plume at a specific location was done with a modified probe (originally designed for particle collection in supersonic regions of the plume) with a tip diameter of 4.5 mm.

Theoretical Background

The light transmittance technique incorporates the use of multiwavelengths of light for continuous transmittance measurements through an exhaust plume containing particles. We ratioed the (ln) values of transmittance to each other, and we then determined the mean particle size (d_{32}) by comparison with Mie theory, which describes the light scattering phenomena.[9]

This procedure was successfully applied by Cashdollar *et al.*[8] to measure the mass concentration and particle size of a cloud of smoke as discussed below. The transmission of light through a cloud of uniform particles is given by Bouguer's law:

$$T = \exp(-QAnL) = \exp\left(-\frac{3QC_mL}{2\rho d}\right). \quad (1)$$

One can use the Mie scattering theory for a single spherical particle to calculate (Q) as a function of particle size, wavelength of light, and complex refractive index of the particle. For polydisperse systems of particles, Dobbins *et al.*[10] showed that Bouguer's transmission law could be written in terms of mean properties:

$$T = \exp\left(-\frac{3\overline{Q}C_mL}{2\rho d_{32}}\right). \quad (2)$$

One can put Eq. (2) into a more useful format by taking the natural log of both sides:

$$\ln T = \overline{Q}\left(-\frac{3C_mL}{2\rho d_{32}}\right). \quad (3)$$

We made multiwavelength transmission measurements over identical path lengths through the exhaust plume. The ratio of the logarithms of the transmittances at any two wavelengths is thus equal to the ratio of the calculated mean extinction coefficients for the same wavelengths:[8]

$$\left[\frac{\ln T(\lambda_i)}{\ln T(\lambda_j)}\right]_{\text{expt.}} = \left[\frac{\overline{Q}(\lambda_i, d_{32}, m)}{\overline{Q}(\lambda_j, d_{32}, m)}\right]_{\text{theor}}. \quad (4)$$

We determined the transmittances experimentally. We used a computer program provided by Cashdollar *et al.*[8] to generate the mean extinction coefficients $\overline{Q}$ and the extinction coefficient ratios ($\overline{Q}_{\lambda_1}/\overline{Q}_{\lambda_2}$) versus d_{32}. These calculations were made for various values of the complex refractive index (m) of the particle, d_{32}, and the geometrical standard deviation (σ_g) of the assumed lognormal particle size distribution. Monomodal log-normal and/or upper-limit distribution functions are often found to apply to clouds of small particles.[6,8] In rocket plumes the distributions are probably bimodal or trimodal.[3,6] At the outer edges of the plume at which small particles are dominant, it was assumed that a monomodal lognormal distribution existed. If the complex refractive index, d_{32}, and the geometrical standard deviation are correct, all the ratios will yield the same particle size (d_{32}) within experimental measurement accuracy. If, however, the distribution is not monomodal lognormal, then the correlation would not occur.

Table 1. Summary of Motor Firings

Run No.	Maximum Pressure (MPa)	Location of Hg Light Beam (mm)
1	2.5	153 from nozzle exit, 25 off centerline
2	2.6	153 from nozzle exit, 25 off centerline
3	2.3	184 from nozzle exit, 25 off centerline

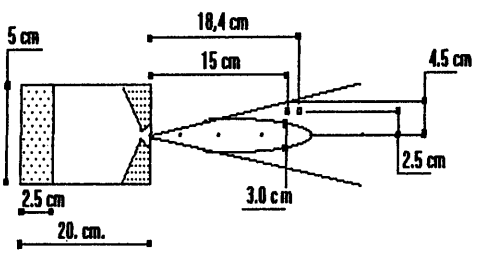

Fig. 1. Configurations of the motor and plume (not to scale).

Table 2. Transmittances (%)

Run No.	Wavelength	λ = 0.365 μm	0.4047 μm	0.4358 μm	0.5461 μm	0.577 μm
1	Transmittance	88.5	91.2	92.5	96.0	96.5
2	Transmittance	89.4	91.9	93.0	96.7	97.1
3	Transmittance	81.0	84.2	86.5	93.4	94.4

If the size of the submicrometer particles thought to be present in the edges of the plume can be assumed to obey a lognormal distribution, then there are four variables that must be determined; d_{32}, σ_g, and the real and imaginary parts of the index of refraction. The latter was assumed independent of λ. Calculations with the Mie code showed that $\overline{Q}$ was insensitive to the absorption index for the expected values between 10^{-2} and zero. Thus for calculation of $\overline{Q}$ the aluminum oxide particles were considered to exhibit no absorption. This resulted in the need for a minimum of three independent log-transmission ratios to determine d_{32}, σ_g, and the refractive index (m).

Experimental Apparatus and Procedures

Rocket Motor

We used an end-burning propellant grain with a 5-cm diameter and 2.5-cm web. The motor chamber length was 20 cm. The propellant was provided by the U.S. Air Force Phillips Laboratory and was a glycidyl azide polymer/ammonium perchlorate propellant containing 4.7% aluminum. The exhaust nozzle had a 45° half-angle converging section, a throat diameter of 0.51 cm, a diverging half-angle of 15° and an area ratio of 3.6. Under those conditions the chamber pressure was approximately 2.5 MPa and the 2–5-μm IR visible length of the plume was approximately 100 nozzle exit diameters.

Collection Probe

The probe was originally designed for collection in supersonic regions of the plume. The probe had a tip (3.3-mm inside diameter) that would swallow, with the aid of an internally supplied annular ejector flow, the gases and the particles at a predetermined location within the plume. The particle collection filter paper had a diameter approximately the same size as the width of the probe body (approximately 22 mm).

Light Transmittance Apparatus

The light sources that we used were a mercury lamp and a helium–neon laser. The collimated white light beam was provided by a 100-W Hg lamp (Oriel Model 6281). The light transmitted through the plume entered a fixed input slit (Oriel Model 77220) that was 25 μm wide and 3 mm high and fell upon the optics inside an Oriel MultiSpec spectrograph (Model 77400). The MultiSpec was designed to be compatible with linear diode array detectors and has a flat focal field for use with diode arrays as long as 25 mm. This instrument has a spectral range of 250–800 nm. We selected gratings that permitted the use of the wavelength band of interest. The photodiode array employed was a Reticon G-series solid-state scanning device. It consisted of 1024 photodiodes on 25-μm centers.[11] The response characteristics of the diode permitted only five of the wavelengths of the Hg source to be detected (0.365, 0.4047, 0.4358, 0.5461, 0.577 μm). We also used an 8-mW He–Ne laser to penetrate the plume. We used the 0.6328-μm wavelength to provide a longer wavelength than that detectable by the Multispec system. We used a Newport photosensor diode with a narrow-pass He–Ne filter to eliminate ambient/plume light.

The five Hg lines provided ten independent ln-transmittance ratios for correlation with the extinc-

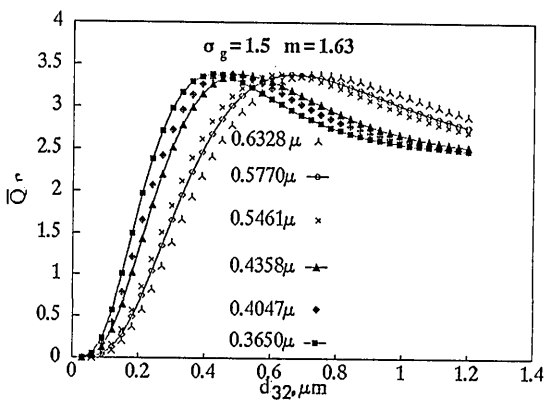

Fig. 2. Extinction coefficients versus the Sauter mean diameter.

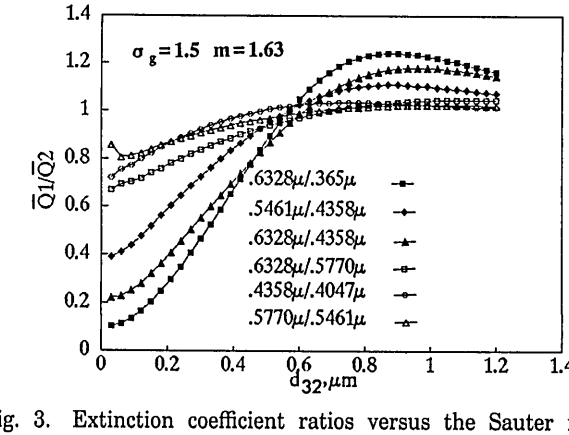

Fig. 3. Extinction coefficient ratios versus the Sauter mean diameter.

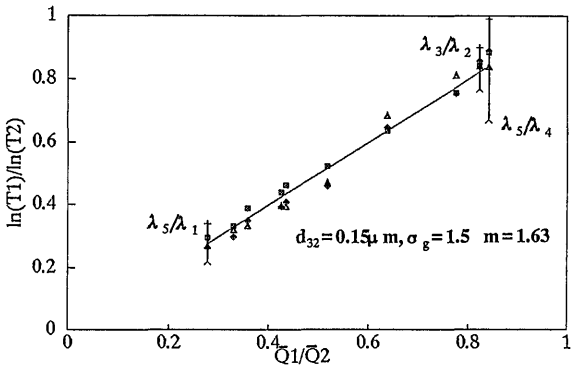

Fig. 4. Log transmission versus extinction coefficient ratios for all runs.

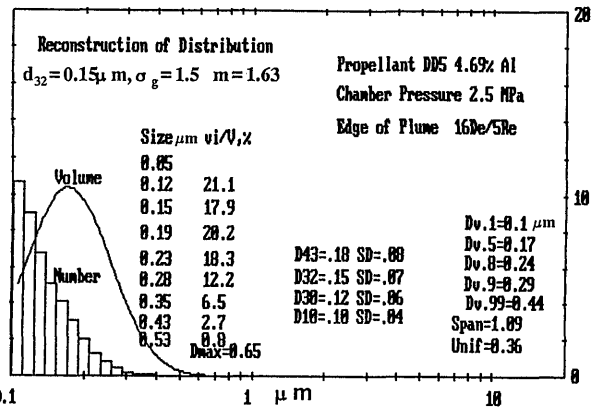

Fig. 6. Reconstructed particle size distribution from the measured Sauter mean diameter (d_{32} = 0.15 μm) and geometrical standard deviation (σ = 1.5).

tion coefficient ratios. Addition of the He–Ne laser increased the number of available ratios to 15. We used a cross pattern so that both light sources would penetrate the same path length in approximately the same plume location.

Data Acquisition and Reduction

A Hewlett-Packard HP9836S computer served as the system controller for the diode array that was used with the white-light source. Data were converted from analog to digital and stored in a HP6942A multiprogrammer. The original data acquisition software[12] was modified. An electrically operated shutter was installed on the outlet of the white-light source. We made eight consecutive scans of the photodiode array in the exhaust with the shutter open, followed by four scans with the shutter closed. The multiple photodiode scans were averaged. We used an IBM PC AT computer to take data from the He–Ne laser. The point during the firing when data were taken was also controlled by the IBM computer. We accomplished this by monitoring the motor chamber pressure (versus time) and by specifying a time delay after steady-state operation was attained. The photodiode array was first aligned so that the five distinct peaks of the mercury light source were correctly positioned. We verified correct system operation by using various neutral density filters. Measurements were first made of the intensities with no particles present in the measurement volume. During the motor firing the transmittances were measured twice, once with the light sources and once without them. We made the latter measurement to determine if significant radiation was emitted from the plume at the wavelengths of the light sources.

Three motor firings were conducted (see Table 1). The exhaust plume was initially video recorded from above with a scaled plate positioned beneath the plume to determine the ideal positioning for the measurements. A sketch of the motor and plume is shown in Fig. 1. An IR camera that had been used in a related investigation[13] was also used to locate the afterburning region and the Mach disk locations within the exhaust plume. It was desired to make the transmission measurements in the outer regions of the plume to reduce the possibility of having large particles present and to be out of the afterburning zone in which high radiation was present. However, it was necessary to be close enough to the exhaust nozzle to provide a relatively steady flow field. The measurement locations were (see Fig. 1) at 16–19 nozzle exit diameters downstream (15–18.4 cm) and 5.25 nozzle exit radii from the plume centerline (2.5 cm).

The computer program provided the extinction coefficients versus d_{32} as a function of geometrical

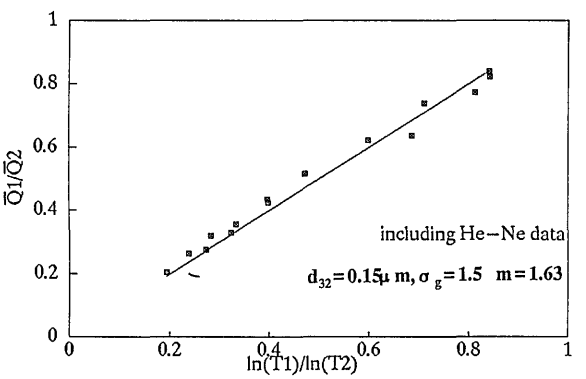

Fig. 5. Log transmission versus extinction coefficient ratios for run 3, including He–Ne laser data.

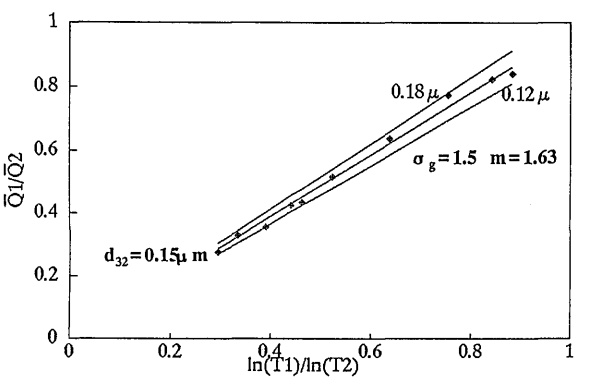

Fig. 7. Data correlation sensitivity for a specified Sauter mean diameter (run 1).

standard deviation (σ_g) and refractive index (m) for each wavelength. We repeated the computations for different values of σ_g, m, and d_{32} until the theoretical extinction coefficient ratios best matched (in the least-squares sense) the measured ln-transmittance ratios.

Results and Discussion

No significant plume radiation was detected at the wavelengths of the illumination sources. Therefore, each run provided two sets of data: one for 100% transmittance (before firing) and the other during firing when particles were present in the plume. Eight scans of the diode array were taken in 0.24 s. Any obviously bad scans were eliminated and the remaining scan voltages were averaged. The wandering of the illuminating beam caused by thermal gradients and flow-field unsteadiness resulted in some fluctuations in both the peak voltages and the diodes on which the peaks occurred. We averaged the peak voltages in order to determine the transmittances presented in Table 2.

Assuming the particle refractive index (real part only) to be independent of the wavelength, we calculated the extinction coefficients (see Fig. 2) and their ratios (see Fig. 3) by using the Mie code[8] for each wavelength. We plotted the ln-transmittance ratios (measured) against the extinction coefficient ratios (calculated) as shown in Fig. 4. Theoretically [see Eq. (4)] the latter graph should be linear with a slope of 45°. To determine the combination of d_{32}, σ_g, and m that gave the best correlation, we applied a regression analysis[14] to best-fit the data by using a linear least-squares fit:

$$R^2 = \frac{\Sigma\,(y_{\text{est}} - \bar{y})^2}{\Sigma\,(y - \bar{y})^2}. \tag{5}$$

A perfect fit would fulfill two conditions: linear criteria (R^2 of unity) and a 45° slope. We varied the particle refractive index from 1.5 to 1.9 and σ_g from 1.3 to 1.7. The calculations of the extinction coefficients were accomplished for all the parameter combinations and for all the wavelengths that were used in the measurement technique, obtaining fifteen ratios for each combination. The use of several wavelengths in a wide band increased the confidence in the correlation. The required accuracy for the measured transmittances increases as λ increases and as the spread between the λ's decreases. This can be seen in Fig. 4. We evaluated the accuracy of the transmittance measurements as approximately 0.5% (from electronic white noises). The resulting uncertainty bands for $\ln\{Tr(\lambda_5)\}/\ln\{Tr(\lambda_1)\}$ are much less than for $\ln\{Tr(\lambda_5)\}/\ln\{Tr(\lambda_4)\}$ at which the wavelengths are much more closely spaced. The difference in wavelengths between λ_5 and λ_4 and between λ_3 and λ_2 is approximately equal (0.031 μm); however, the ln-transmittance ratios for the lower wavelengths result in less uncertainty because of lower values of transmittance.

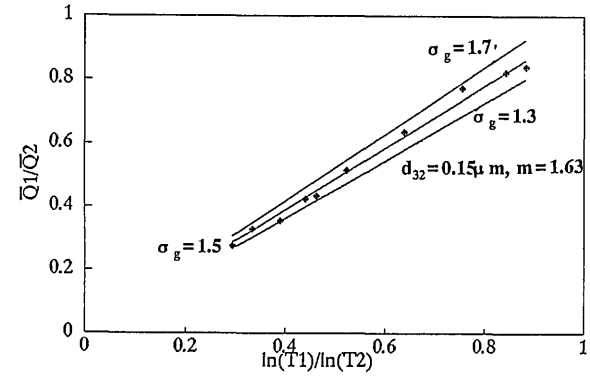

Fig. 8. Data correlation sensitivity for a specified geometrical standard deviation (run 1).

The best correlation (from a least-squares and 45° slope standpoint) was obtained (see Figs. 4 and 5) for a Sauter mean diameter of 0.15 μm with a geometrical standard deviation of 1.5 and an index of refraction of 1.63. Figure 4 shows good test-to-test repeatability, and the results shown in Fig. 5 added confidence in the data by obtaining the same correlation while the wavelength band was substantially increased. Assuming a lognormal distribution, we retrieved the particle size distribution (by using the statistical functions) shown in Fig. 6. The latter shows that particles as large as 0.65 μm were present in the measurement volume and that 50% of the particle volume was concentrated in particles smaller than 0.17 μm. The mean diameter d_{30} was only 0.12 μm, indicating that most of the particles (98% of the total number of particles) were smaller than 0.15 μm.

Once the combination was obtained for the best agreement between the calculated extinction coefficient ratios and the measured ln-transmittance ratios, we performed an analysis to obtain the sensitivity of the correlation to each of the parameters. We accomplished this by perturbing the value of each parameter independently around its nominal value and by observing the induced changes to R^2 and the slope of the least-squares fit that passed through the origin (desired to be 45°). Figures 7–9 present the

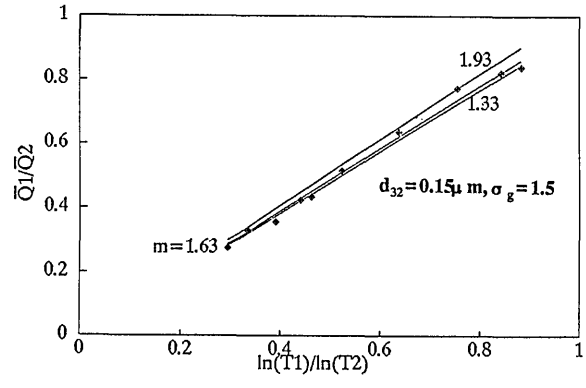

Fig. 9. Data correlation sensitivity for a specified index of refraction (run 1).

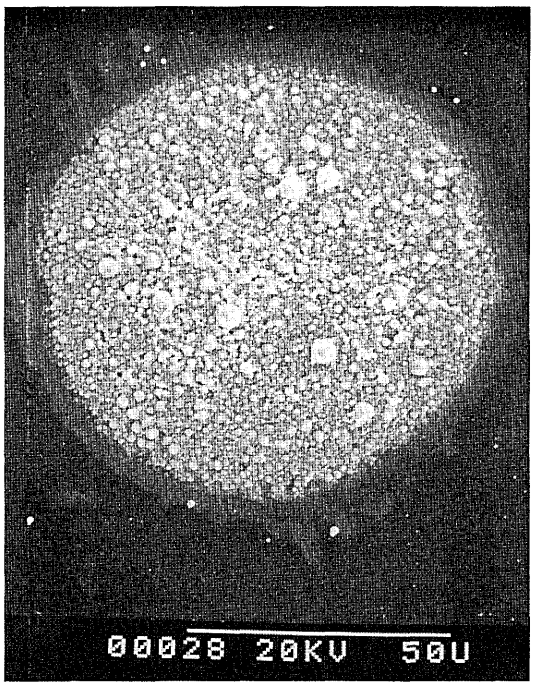

(a)

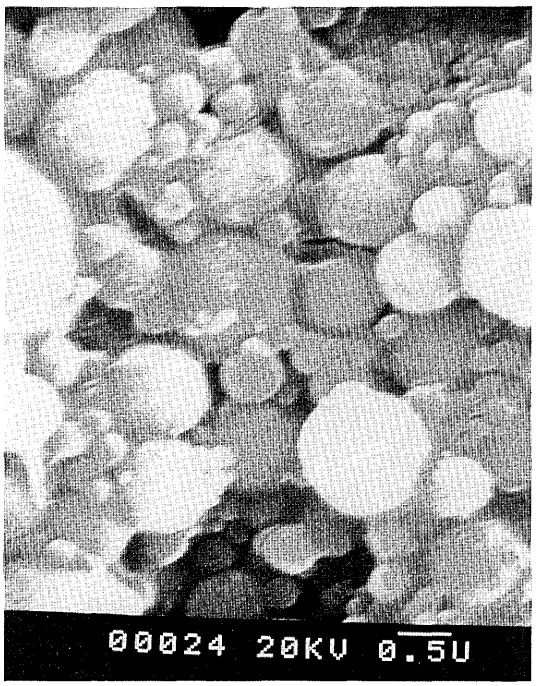

(b)

Fig. 10. Scanning electron microscope pictures of collected particles: (a) conglomerate droplet (magnification 900×), (b) alumina particle size distribution (magnification 18,000×).

results of the analysis. Forcing the lines, which represent the correlation, to pass through the axes origin and allowing a maximum variation of 1% in the slope led to an estimation of the absolute errors of each parameter that would give a good correlation. The results obtained were

$$d_{32} = 0.150 \pm 0.006\ \mu\text{m},$$

$$\sigma_g = 1.50 \pm 0.04,$$

$$m = 1.63 \pm 0.13.$$

It appears that this technique is much more sensitive to the particle size distribution than to the index of refraction. The obtained refractive index was in the range as reported elsewhere[7] (between 1.5 and 1.8) with a clear tendency toward the value of 1.63, near to that reported for pure gamma-phase alumina (1.665). The probe that we used to collect particles in the edge of the plume used a cold ejector gas. The collected exhaust products showed evidence of condensed water/HCl droplets containing many small Al_2O_3 particles. The size of these droplets was between 10 and 50 μm. These droplets were large, even for secondary smoke (plume H_2O/HCl condensation) in which most particles are submicrometer in size (0.01–0.5 μm). Thus, the condensation into large agglomerates probably occurred within the probe. In addition, if many plume particles were contained in these large droplets, the extinction data would not have correlated as discussed above. Each droplet contained millions of small particles. A detailed analysis of the magnified pictures (by using a scanning electron microscope, SEM Hitachi S-450, with magnification as high as 20,000×) revealed (see Fig. 10) that one agglomerate contained two particles of 5-μm diameter, six particles of 3.5 μm, approximately 5000 particles of 2 μm, greater than 10^5 particles of 1.0 μm, approximately the same number for a 0.5-μm particle diameter, and millions of particles with an apparent diameter of less than 0.25 μm. To an order of magnitude, these figures will give a mean diameter between 0.2 and 0.3 μm. Because of the limitations of the picture reduction technique, statistical misrepresentation, limited observable lower size, and human errors, these results were only qualitative; yet they reinforced the optically obtained results.

It should be added that the assumed lognormal distribution was successful in correlating the data from the particles flowing in the edge of plumes. Nevertheless, a question arises about how the presence of very few particles as large as 5 μm could affect the transmittance measurements. Calculations based on Eq. (2), the definition of the Sauter mean diameter, and Mie code values for Q_{ext} showed that, if 5-μm particles are present with 0.1-μm particles, the measured transmittance and the calculated d_{32} will not be affected if the volume of the smaller particles is at least 2.5 times the volume of the larger particles. This implies that the number of the small particles should be greater than half a million times the number of the large particles. This number ratio was, as mentioned before, evidenced by the SEM pictures. It is, therefore, possible to find a few larger particles in the plume edges and yet to represent the particle population as presented in Fig. 6.

Conclusions

The results of this investigation have shown that the multiple-wavelength transmission measurement technique can be used to obtain the Sauter mean diameter and the particle size distribution (assumed to be lognormal) of the small particles present in the edge of a solid rocket motor plume. The data reduction method has been shown to be more sensitive to changes in the Sauter mean diameter than to the index of refraction. The values measured for Al_2O_3 particles in the edge of the plume were $d_{32} = 0.150 \pm 0.006$ μm, $\sigma_g = 1.50 \pm 0.04$, and $m = 1.63 \pm 0.13$. The good correlation of the data indicated that submicrometer particles were dominantly present at the edge of the plume. This was also in reasonable agreement with the size distribution of collected particles. The nominal index of refraction of 1.63 also indicated that the particles were probably gamma-phase Al_2O_3, although measurement accuracy prevented a definite conclusion.

Appendix A: Nomenclature

A is the cross-sectional area of a particle,
Cm is the mass concentration of particles,
d is the particle diameter,
d_{32} is the Sauter mean diameter,
L is the path length containing particles,
m is the index of refraction of particle,
n is the number concentration of particles,
Q is the dimensionless extinction coefficient,
$\overline{Q}$ is the mean extinction coefficient,
R^2 is the coefficient of determination, Eq. (5),
T is the transmittance,
λ is the wavelength,
ρ is the particle density, and
σ_g is the geometrical standard deviation.

This investigation was supported by the U.S. Air Force Phillips Laboratory, Edwards Air Force Base, California, under contract MIPR F04611-91-X-0004 and by the National Research Council.

References and Notes

1. S. M. Dash, "Analysis of exhaust plumes and their interaction with missile airframes," in *Tactical Missile Aerodynamics,* M. J. Hemsch and J. N. Nielsen, eds., Vol. 104 of AIAA Progress in Astronautics and Aeronautics (American Institute of Aeronautics and Astronautics, Inc., New York, N.Y., 1986), pp. 778–851.
2. C. J. Hwang and G. C. Chang, "Numerical study of gas-particle flow in a solid rocket nozzle," AIAA J. **26,** 682–689 (1988).
3. L. D. Strand, J. M. Bowyer, G. Varsi, E. G. Laue, and R. Gauldin, "Characteristics of particles in the exhaust plume of large solid-propellant rockets," J. Spacecraft **18**(4), 297–305 (1981).
4. H. Cheung and N. S. Cohen, "Performance of solid propellants containing metal additives," AIAA J. **3,** 250–257 (1965).
5. K. M. Dill, R. A. Reed, V. S. Calia, and R. J. Schultz, "Analysis of crystalline phase aluminum oxide particles from solid propellant exhausts," J. Propulsion Power **6,** 668–671 (1990).
6. R. A. Dobbins and L. D. Strand, "A comparison of two methods of measuring particle size of Al_2O_3 produced by a small rocket motor," AIAA J. **8,** 1544–1550 (1970).
7. R. B. Lyons, J. Wormhoudt, and J. Gruninger, "Scattering of radiation by particles in low altitude plumes," presented at the American Institute of Aeronautics and Astronautics 16th Thermophysics Conference.
8. K. L. Cashdollar, C. K. Lee, and J. M. Singer, "Three-wavelength light transmission technique to measure smoke particle size and concentration," Appl. Opt. **18,** 1763–1769 (1979).
9. H. C. van de Hulst, *Light Scattering by Small Particles* (Dover, New York, 1981), Chap. 9.
10. R. A. Dobbins, L. Crocco, and I. Glassman, "Measurement of mean particle sizes of sprays from diffracatively scattering light," AIAA J. **1,** 1882–1886 (1963).
11. EG&G Reticon, "Spectral response of reticon linear photodiode arrays," Application Note 121 (EG&G Reticon, Sunnyvale, Calif., 1980).
12. R. K. Harris, "An apparatus for sizing particulate matter in solid rocket motors," M.S. thesis (Naval Postgraduate School, Monterey, Calif., 1984).
13. D. Laredo, J. D. McCrorie II, J. K. Vaughn, and D. W. Netzer, "Motor and plume particle size characteristics for solid propellant rocket motors," submitted to J. Propul. Power.
14. M. R. Spiegel, *Probability and Statistics* (McGraw-Hill, New York, 1990), pp. 263–265.